Science of the Total Environment 929 (2024) 172559

Contents lists available at ScienceDirect

Science of the Total Environment

journal homepage: www.elsevier.com/locate/scitotenv

Modelling pesticide degradation and leaching in conservation agriculture: Effect of no-till and mulching

Jeanne Vuaille [a,*], Per Abrahamsen [a], Signe M. Jensen [b], Efstathios Diamantopoulos [c], Tomke S. Wacker [b], Carsten T. Petersen [a]

[a] Department of Plant and Environmental Sciences, University of Copenhagen, Thorvaldsensvej 40, 1871 Frederiksberg, Denmark
[b] Department of Plant and Environmental Sciences, University of Copenhagen, Højbakkegård Alle 30, 2630 Taastrup, Denmark
[c] Chair of Soil Physics, University of Bayreuth, Universitätsstr. 30, 95447 Bayreuth, Germany

HIGHLIGHTS

- A new mulch module in Daisy allows to describe Conservation Agriculture (CA) effects.
- Two scenarios were simulated: one under CA and one with conventional tillage (CT).
- Pesticide leaching to drains was not systematically different between CA and CT.
- Pesticide degradation and sorption in mulch and soil showed vertical heterogeneity.
- Global sensitivity analyses identified 7 parameters out of 25 to improve simulations.

GRAPHICAL ABSTRACT

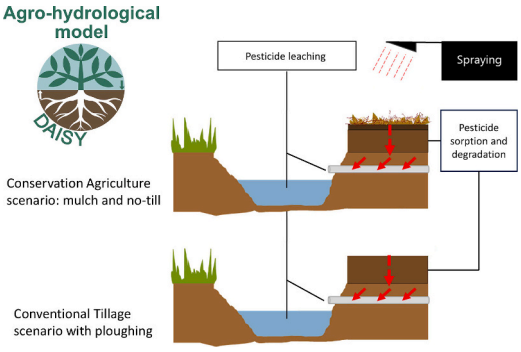

ARTICLE INFO

Editor: Daniel Wunderlin

Keywords:
Conservation agriculture
Mulch
No-till
Biopores
Drains
Daisy model

ABSTRACT

No-till and mulching are typical management operations in conservation agriculture (CA). To model pesticide degradation and leaching under a CA scenario, as compared to a conventional-tillage scenario (CT), the mulch module of the agro-hydrological model Daisy was extended. A Daisy soil column was parameterized with measurements of topsoil, mulch, and a realistic subsoil, and tested against published experimental data of pesticide fate in laboratory soil columns covered by mulch. Uncertainty and sensitivity analyses of the new Daisy version were conducted for a series of weather, soil, pesticide, and mulch parameters, using 4939 Monte Carlo simulations under each scenario. Results showed that there was no systematic difference in pesticide leaching from the topsoil (to the subsoil and directly to drains via drain-connected biopores) between CA and CT, but pesticide degradation and sorption were significantly different; degradation in the mulch and uppermost soil surface layer (0–3.5 cm) was larger in CA while degradation was larger in CT when considering the whole topsoil (0–30 cm). This difference for the whole topsoil could be explained by pesticide interception in CA in the part of the mulch not in direct contact with the soil where degradation is assumed not to occur. The sensitivity analysis highlighted non-influential parameters and seven parameters out of twenty-five to be better estimated to improve the accuracy of the predictions.

* Corresponding author.
E-mail address: jeannev@plen.ku.dk (J. Vuaille).

https://doi.org/10.1016/j.scitotenv.2024.172559
Received 10 October 2023; Received in revised form 28 March 2024; Accepted 16 April 2024
Available online 17 April 2024

1. Introduction

Conservation agriculture (CA) has gained in popularity in Europe over the past 10 years as a sustainable cropping system, following a global trend. According to Kassam et al. (2019), the cultivated area under CA in the world increased by 29 % from 2010 to 2015 reaching 12.5 % of the global cropland. CA can be described by three main principles (FAO, 2022): i) minimum mechanical soil disturbance or no-till, ii) permanent soil organic cover through the introduction of cover crops and mulching (minimum 33 % of soil surface covered by crop residues), and iii) species diversification by implementing crop rotations with diversified cover crops (FAO, 2021). Adopting these principles often leads to a lower workload and fuel consumption, a reduction in soil erosion, and a potential for carbon sequestration in the surface soil layer. However, little is known about the effect of CA conversion on pesticide fate, especially about the effect of mulching and no-till.

Soil erosion is reduced due to greater aggregate stability, less gravity-driven soil movement, and larger (macro) porosity and infiltrability in the topsoil. Such soil structural and hydraulic properties result from the higher inputs of fresh organic matter on the soil surface e.g., mulch, which soil organisms and especially earthworms feed on (Scopel et al., 2013). This biological activity promotes the creation of vertical, continuous and rather permanent burrows in CA (Alletto et al., 2010), compared to CT where macropore continuity is frequently broken by tillage. A greater soil organic matter content in the surface layer can also increase the water-holding capacity of the soil, and thereby lower the air space available to rapidly absorb rainwater. When combined with an enhanced surface-connected macroporosity in CA, preferential flow may be triggered to a larger extent than in a ploughed field (Jarvis, 2007; Petersen et al., 2001). This is particularly important for drained agricultural fields with subsurface tile drains, as earthworm channels near the drain lines have been shown to establish direct connections between the drains and the soil surface (Nielsen et al., 2015; Petersen et al., 2012). Hence, preferential flow through surface- and drain-connected biopores in CA may lead to more pesticide leaching to subsurface drain lines than in CT (Reichenberger et al., 2007).

On the other hand, the presence of mulch and structurally stable soil surface in CA can prevent the soil from sudden saturation and preferential flow. In their study, Findeling et al. (2007) estimated a storage capacity of 0.8 and 1.2 mm for rye and rape residues, respectively, showing the ability of mulch residues to store the water from small rain events. Pesticides can also be intercepted by the mulch so that their transfer to the soil surface is reduced or retarded, according to their sorption properties to organic carbon. In a soil column experiment, Aslam et al. (2015) showed that a mulch of maize and dolichos intercepted and retained via sorption approximately 56 % of the pesticide s-metolachlor and 48 % of the glyphosate. Cassigneul et al. (2015) measured sorption coefficients, K_d, of glyphosate in several types of cover crops less than half that observed for s-metolachlor. Likewise, pesticides sorbing to organic carbon may be retained in the uppermost soil layer in CA because of the high organic matter content. This may thus decrease their mobility in soil, while non-sorbing pesticides may be degraded faster in the uppermost soil layer due to high microbial activity (Henneron et al., 2015; Levanon et al., 1993; Wacker et al., 2022). In addition, previous work has demonstrated that the triggering of biopore flow and infiltration in biopores can be particularly high in areas with structurally damaged soil due to traffic of heavy machinery in CT (Vuaille et al., 2021).

Modelling is an essential tool to predict pesticide fate under a large number of weather and field conditions. In particular, modelling simultaneously pesticide and water dynamics in a soil subject to no-till and mulching would help unravel the effect of CA on pesticide fate. In the European Union registration process for plant protection products, a modelling procedure is integrated to estimate the predicted environmental concentrations of pesticides, based on realistic application scenarios described in the Generic guidance for FOCUS surface water Scenarios (FOCUS, 2001). The procedure includes models that simulate pesticide transport through surface run-off as affected by rainfall intensity, slope, soil roughness and cover (the pesticide root zone model (PRZM), Suárez, 2005) and subsurface drain lines (MACRO, Jarvis and Larsbo, 2012). Nevertheless, apart from a surface run-off reduction in PRZM, these models do not account for the effect of crop residues on the water and pesticide dynamics in soil.

Lammoglia et al. (2017) used a combination of the models STICS (Brisson et al., 1998) and MACRO to simulate crop growth and pesticide fate in diverse cropping systems that also include mulching. Their sensitivity analysis showed that the presence of a mulch at a density of 10 t ha^{-1} could significantly increase the cumulated amount of percolated water down to 1 m depth and pesticide leaching compared to simulations with bare soil due to reduced soil evaporation and surface run-off and thus a promotion of water storage and infiltration. However, the model setup considered neither pesticide interception and degradation capacity in the mulch, nor the enhanced microbial activity due to mulching. Marín-Benito et al. (2018) also used MACRO to model s-metolachlor fate in CA. Their approach to simulate the presence of a mulch consisted in parameterizing a pure sandy soil layer of 5 cm at the top of the soil column, with structural and hydraulic properties corresponding to a highly organic soil layer, combined with reduced soil evaporation calibrated to field data. Both pesticide degradation and sorption were simulated in the mulch layer. Predictions of water percolation, soil temperature and herbicide leaching appeared satisfactory compared to the field observations, which however was not the case for predictions of the soil water content. In addition, the study remained limited to the specific case of naturally drained soil. Aslam et al. (2018) simulated the interception, sorption, leaching, and degradation of s-metolachlor and glyphosate in laboratory soil columns covered by mulch with the mechanistic model PASTIS (Garnier et al., 2003). The model predictions showed a good agreement with the measurements. Their results revealed that high and infrequent rain increased pesticide wash-off from mulch, while low and frequent rain stimulated pesticide biodegradation due to a higher soil water content. Yet, these simulations represented laboratory conditions and did not consider the presence of macropores and drains.

The mechanistic model Daisy developed for flat agricultural fields (Abrahamsen and Hansen, 2000; Hansen et al., 2012a) can be used to simulate pesticide leaching (Hansen et al., 2012b) and in particular leaching to drains (Holbak et al., 2022). The Richards and advection-dispersion equations are used for calculating water and solute transport in the soil (Mollerup et al., 2014). The heat flow is calculated with the conduction-convection equation (Abrahamsen and Hansen, 2000). Pesticide degradation in the soil is described by first-order kinetics and is affected by soil temperature, pressure potential, and depth. Pesticide sorption to soil particles can be assumed instantaneous using isotherm models or time-dependent using sorption kinetics. Daisy includes a biopore model (Holbak et al., 2021), which simulates preferential flow and solute transport in macropores. The term biopore is used as these macropores mostly refer to those biologically formed i.e., earthworm burrows and root channels. Such biopores can be parameterized based on direct field measurements (Nielsen et al., 2015; Petersen et al., 2012). In addition, Daisy has a dynamic crop module (Gyldengren et al., 2020), which allows simulating different growth conditions as affected by weather and soil properties.

Along with an organic matter model describing multiple pools for soil microbial biomass and soil organic matter, Daisy can simulate different farming practices and their effects on water and nutrient dynamics (Abrahamsen et al., 2010; Bruun et al., 2003).

With these characteristics, Daisy includes a large number of parameters describing, among others, the soil column, weather characteristics, crops, pesticides, and tillage type. To determine the influence of specific parameters on model predictions, sensitivity analyses are generally carried out varying one parameter at a time (Saltelli et al., 2010). However, this method does not account for potential interactions

between parameters. Global sensitivity analysis (GSA) methods, on the other hand, offer the possibility to estimate the influence of a multitude of parameter combinations on predictions, and therefore to calculate the influence of parameters both through their individual and through combined effect (Saltelli et al., 2008). No GSA has yet been performed for Daisy on pesticide leaching and degradation.

The objective of the present study was twofold (Fig. 1A). Based on a new mulch module in Daisy, the first objective was to compare pesticide leaching and pesticide degradation amounts as simulated by Daisy between a CA and a conventional tillage (CT) scenario. The two cropping scenarios were described with specific topsoil measurements. Pesticide leaching refers in the following to leaching from the topsoil to the subsoil (leaching from 30 cm depth) or from the topsoil directly to the drains through biopore flow.

Second, the sensitivity of the simulated leaching and degradation towards a series of parameters was investigated, to determine which ones had the highest influence on the predictions and should therefore be better estimated. The hypotheses were that pesticide leaching to the subsoil and drains would be similar in CA and CT despite the higher density of biopores in CA, due to more pesticide interception, sorption and degradation in mulch and soil surface in the CA system.

The Daisy model and the extension of the mulch module to simulate water and pesticide dynamics in mulch e.g., interception, retention, degradation and wash-off, based on PASTIS mulch module (Aslam et al., 2018; Findeling et al., 2003, 2007; Garnier et al., 2003) are first presented. The laboratory and field measurements used to fit new parameters via inverse modelling, test the new Daisy mulch module and parameterize Daisy for CA and CT scenarios (Fig. 1A, steps 1 and 2) are then described. Second, the modelling setup used to conduct uncertainty analysis and GSA with Sobol indices (Saltelli et al., 2008) for a series of soil, mulch, pesticide and weather parameters – including the newly integrated parameters (Fig. 1A, steps 2 and 3) – are introduced. Thousands of simulations are run with unique combinations of parameter values for the uncertainty analysis and used subsequently for calculating Sobol sensitivity indices. These indices are used to estimate 1) which parameters should be better measured or estimated due to their relatively high influence on the predictions of leaching and degradation, but also 2) which parameters can be fixed to any value in their distribution due to their negligible direct or indirect influence on the output variable.

At last, the mulch module test against experimental data and the

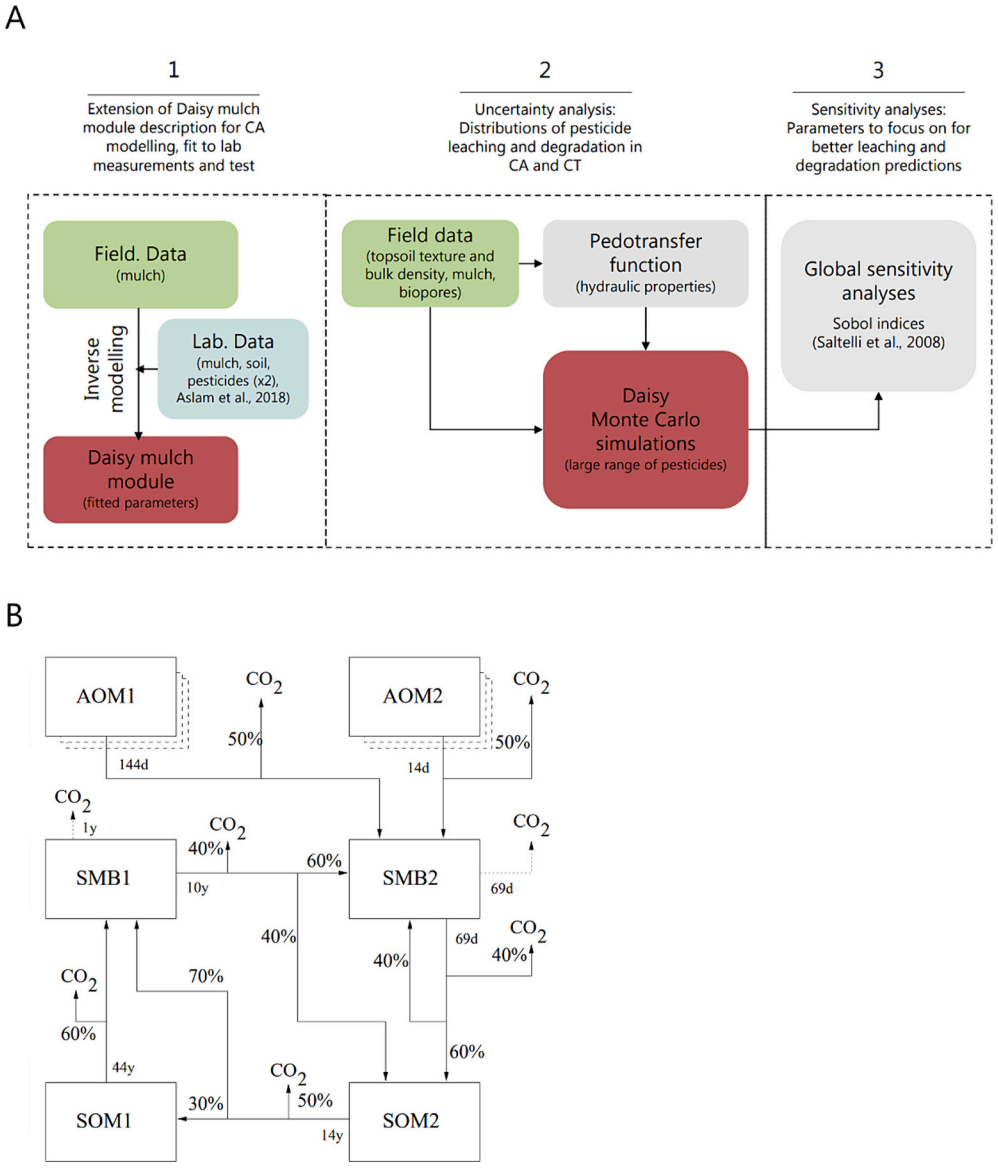

Fig. 1. Material and methods overview. A: Extension of Daisy mulch module, uncertainty and sensitivity analyses. B: Standard organic matter model in Daisy (Abrahamsen et al., 2010, unpublished manuscript).

results of the simulations are presented and discussed.

2. Material and methods

2.1. The Daisy model

2.1.1. Tillage operations in Daisy

Tillage in Daisy is implemented to have three effects: 1) removing any crops on the field, 2) incorporating a fraction of the organic matter from the surface into the soil at a given depth, and 3) homogenizing the content of the soil in the affected depth e.g. soil water content and organic matter contents. Under the CT scenario the specific "ploughing" operation is used, where two soil intervals (named top and bottom) are homogenized and then swapped. The content of the top interval results at the bottom, and vice versa.

2.1.2. Daisy's organic matter model

The organic matter model in Daisy is described by three compartments (Fig. 1B): *1)* the added organic matter (AOM), which describes fresh organic material such as crop residues, organic fertilizers and rhizodeposition, *2)* the soil microbial biomass (SMB), which corresponds to the living microbial compartment, and *3)* the soil humus named soil organic matter (SOM), which describes humified organic matter. These AOM, SMB and SOM compartments are by default divided into two pools. Each pool is defined by a specific size (g C cm^{-3} soil), turnover rate (d^{-1} or y^{-1}), efficiency rate (% of carbon dioxide released during turnover) and carbon:nitrogen (C:N) ratio (Fig. 1B). In each compartment, the first pool (AOM1, SMB1, SOM1) is characterized by a slow turnover rate compared to the second pool (AOM2, SMB2, SOM2). Each source of added organic matter is represented by a separate set of AOM pools, so the total number of AOM pools in the system is variable. Fresh organic matter added to the soil through fertilization and crop residues, including dead leaves from the cultivated crops, first reach the soil surface. From the soil surface, it is bioincorporated by earthworms at a certain speed (g dry mass m^{-2} h^{-1}) and can be incorporated by soil tillage. Bioincorporation is affected by the C:N ratio of the organic matter. Soil tillage uniformly distributes soil organic matter in the tilled layer. AOM pools are thereafter degraded by SMB2. As living pools, both SMB1 and SMB2 have maintenance rates that relate to the fraction degraded to maintain the organisms' functions (h^{-1}). When degrading, SMB2 is transformed into SOM2 while a fraction returns to the pool. While SOM and SMB pools are only defined in the soil, AOM pools have an optional above-ground component. These constitute a mulch layer in the model that influences water and pesticide interception and evapotranspiration. Soil and surface degradations of AOM pools in Daisy follow first-order reaction kinetics and are affected by soil water pressure potential, temperature as well as N availability (Hansen et al., 1991).

The division between AOM1 and AOM2 and their properties can be determined by lab incubation experiments for specific types of added organic matter. The properties of the SMB and SOM pools have been determined by a combination of short-term (Mueller et al., 1997) and long-term experiments (Bruun et al., 2003).

2.2. New mulch module

Daisy mulch biomass consists of the above-ground part of all the AOM pools (Fig. 1B). In the present study, the mulch module was improved based on PASTIS mulch module described in Aslam et al. (2018) and Findeling et al. (2007) and using PASTIS methods available in the Virtual Soil platform (Lafolie et al., 2014). The objective was to describe organic matter, water and pesticide dynamics in mulch and soil with fewer and less site-specific parameters in order to develop a more generalizable module. As such, Daisy mulch was developed as a one-layer mulch compared to the two layers in PASTIS.

2.2.1. Mulch organic matter

The new Daisy mulch is composed of one layer of which the structure is characterized by a *height* (cm) (Eq. (1)) and a mulch *cover* (−) (Eq. (2)). *height* and *cover* are derived from a variable dry mass, *DM* (g cm^{-2}), and three user-defined parameters i.e., the mulch bulk density, ρ_{bm} (g cm^{-3}), the specific mulch area index, *SpMAI* (cm^2 g^{-1}), and an extinction coefficient, γ (−).

$$height = \frac{DM}{\rho_{bm}} \tag{1}$$

$$cover = 1 - e^{-\gamma\ SpMAI\ DM} \tag{2}$$

Mulch residues in Daisy first degrade to form dissolved organic matter (DOM) as described in Garnier et al. (2003). DOM is characterized by C and N contents also referred to as DOC and DON, respectively. DOM is transported from mulch to soil via wash-off (2.2.3) where it is further degraded. DOM does not impact pesticide transport via sorption.

Mulch decomposition to DOM in Daisy is based on the same description of decomposition by SMB2 as the surface AOM pools (2.1.2) multiplied however by a microbial factor f_b (−):

$$\frac{dAOM_{surface}}{dt} = -f_b f_h f_T f_N AOM_{surface}(t) \tag{3}$$

With f_h, f_T, and f_N the soil water pressure potential, temperature as well as N availability factors (Hansen et al., 1991). f_b is inspired by Michaëlis-Menten reaction kinetics (Garnier et al., 2003) such as:

$$f_b = \frac{SMB_{ref} + K_M}{SMB_{ref}} \frac{SMB2}{SMB2 + K_M} \tag{4}$$

With SMB_{ref} (g C cm^{-3}) a specific reference C content of the SMB pool, *SMB*2 (g C cm^{-3}) the active soil organic biomass, assumed to decompose AOM, and K_M (g C cm^{-3}) a Michaëlis-Menten constant for the decomposition of AOM. If *SMB*2 equals SMB_{ref}, f_b becomes 1. Mulch decomposition is set to only occur in the part of the mulch in direct contact with the soil and its microorganisms. This is estimated to correspond to 20 % of the height of the mulch based on PASTIS description (Aslam et al., 2018).

In the present study, SMB_{ref} was set equal to K_M, making f_b equal to 1 for a *SMB*2 as large as the K_M constant value (Eq. (4)). This reflects the assumption that under favourable conditions, the microbial factor is not smaller than 1. Factor f_b (Eq. (5)) thus tends towards 0 for very large K_M values and towards 2 for a K_M value equal to 0. The considered SMB2 pool is from the soil layer Δz_M (cm) affecting processes in the mulch layer (where residues are in direct contact). Δz_M is set to 5 cm depth in this study, which reflects observations from laboratory studies (Aslam et al., 2018; Findeling et al., 2007).

$$f_b = 2\frac{SMB2}{SMB2 + K_M} \tag{5}$$

2.2.2. Mulch water

Water retention in the mulch layer is described by Eq. (6):

$$w(h) = w_R + (w_M - w_R)e^{kh} \tag{6}$$

where $w(h)$ (g g^{-1}) corresponds to the gravimetric water content at a soil water pressure head h (cm), w_M (g g^{-1}) the maximal water content, w_R (g g^{-1}) the residual water content, and k (cm^{-1}) the exponential curve parameter.

Water interception by the mulch layer is described in Eq. (7) as dependent on the amount of water already retained by the mulch, w, the maximal and residual water contents, w_M and w_R:

$$I_{mulch\ water} = rain\ cover\ e^{-\alpha\frac{w_M - w_R}{w_M - w}},\ if\ w < w_M \tag{7}$$

$$I_{mulch\ water} = 0,\ if\ w = w_M$$

where $I_{mulch\ water}$ (mm h^{-1}) represents the amount of water being intercepted by the mulch, *rain* (mm h^{-1}) the amount of water falling on the ground, *cover* the mulch cover defined in Eq. (2), and α (−) the mulch water recharge capacity as also defined in Findeling et al. (2007). Water falling on mulch but not stored percolates through the mulch layer and reaches the soil. Water evaporation occurs on mulch and on the proportion of soil not covered by mulch.

In addition, water can move between the mulch layer and the soil by capillarity according to the Darcy's flow equation (q, cm h^{-1}, Eq. (8)), based on the hydraulic conductivity of the soil surface, $K(h)$ (cm h^{-1}), the differences of hydraulic potential and height between mulch and soil surface (Δh and Δz_M in cm, respectively), and an exchange factor f_e (−) describing the continuity between mulch and soil:

$$q = -K(h)\frac{\Delta h}{\Delta z_M} f_e \quad (8)$$

where Δh is the difference between the water pressure in the mulch (Eq. (6)) and the water pressure in the middle of the soil layer affecting processes in the mulch layer, defined as Δz_M (2.2.1).

2.2.3. Pesticides and other chemicals in mulch

When sprayed on the field, pesticides are intercepted by mulch according to its soil cover. During rainfall, if the mulch water content reaches a given saturation index Si (%), pesticides can diffuse from mulch water to the percolating rainwater and thereby enter the soil surface through wash-off according to the mulch mass exchange rate, E_p (h^{-1}) in Eq. (9), as also described in Aslam et al. (2018).

$$I_{mulch\ pest} = -E_p C_{pest} \quad (9)$$

With $I_{mulch\ pest}$ (g g^{-1} h^{-1}) being the quantity of pesticide intercepted by the mulch and C_{pest} (g g^{-1}) the pesticide content in the mulch water.

Pesticides stored in mulch are also subject to degradation based on the percentage of mulch in contact with the soil (20 % of the dry mass according to Aslam et al., 2018) and the amount of wash-off during rainfall. Pesticide degradation is assumed to occur through co-metabolism. In a co-metabolic transformation, the soil microbial biomass growing during mulch decomposition can fortuitously transform pesticides (Bollag and Liu, 1990; Aslam et al., 2018). Pesticide degradation in Daisy follows first-order reaction kinetics and is affected by soil water pressure potential, temperature and depth (Abrahamsen and Hansen, 2000). In this new version, it is also subjected to the microbial factor f_b (Eq. (4)) to account for co-metabolism. In Daisy mulch module, pesticide and mulch degradations are thus controlled by the same microbial biomass (SMB2 pool) and occur simultaneously. The K_M factor in Eq. (4) might differ between pesticides and organic residues, as the increase in SMB2 might not necessarily affect equivalently the degradation of mulch and pesticide. They are therefore labelled K_{MM} and K_{MP}, respectively.

Pesticide sorption to soil and organic matter is assumed instantaneous using the linear Freundlich isotherm (Table 2 and Table 3) and does not affect pesticide degradation.

2.3. Field experiment

2.3.1. Experimental layout

The monitored fields were part of a 4-year project (2017–2020), which investigated the environmental effects of CA. Two farms located on Zealand, Denmark, and separated by about 2 km were selected. The two farms represent two different cropping systems, CT with ploughing and CA. The investigated fields in both farms are characterized by a loamy texture and present a plough pan at 25 cm depth (Table 1). At the CT farm, annual mouldboard ploughing has been conducted for at least 30 years to cultivate commonly grown crops like barley, wheat and rape along with harrowing at about 5 cm depth. At the CA farm, crops have been cultivated without ploughing since 2000, but no-till combined with CA principles have been applied since 2011, developing a surface horizon rich in organic matter down to 3.5 cm. Thus, the investigated fields presented physical characteristics typical of the CA and CT systems.

During the 4 years of the project, a 2-year crop rotation *winter wheat–spring barley* was implemented on both fields with cover crop mixtures composed of vetch, oilseed radish, and oat placed between all cereal crops. On each field, soil plots were established according to a randomised complete block design with four blocks each containing four cover crop treatments, namely "no cover crop", "vetch and oat", "vetch and oilseed radish" and "oilseed radish".

2.3.2. Soil data

Soil texture was determined at 15–20 cm depth ($n = 16$) on both field sites (Table 1) by a combination of sieving and sedimentation as described by Gee and Or (2002), and soil organic matter at two depths i.e., 0–3.5 and 15–20 cm ($n = 32$), by the loss-on-ignition method (Nelson and Sommers, 1996).

Undisturbed soil core samples of 100 cm^3 were collected five times between 2017 and 2019 – three times in autumn and twice in spring (although not all depths of the topsoil were equally sampled). Sampling was performed in triplicates in each block, from 2 cover crop treatments "without cover crop" and "vetch and oat", in full-N fertilization plots, and at three depths i.e., 0–3.5 ($n = 224$ for five sampling series in each cropping system), 15–20 ($n = 192$ for four sampling series) and 25–30 cm ($n = 54$ for one sampling series in each system). Samples with continuous macropores were discarded in the field based on visible inspection. This resulted in 470 samples in total, stored at 4 °C until analyzed in the laboratory.

The cores were saturated from below with de-aired tap water on a sand table and then equilibrated at 100-hPa suction. The equilibrium water content M_w (representing field capacity for this soil type) was measured. The samples were subsequently dried at 105 °C to obtain the dry bulk density ρ_b (g cm^{-3}). The density of drain-connected biopores was estimated in September 2020 at the CA farm on a nearby field using the smoke injection technique described by Petersen et al. (2012). A drain line of 14 m was investigated and smoke-emitting biopores were reported according to their distance from the smoke-injected pipe.

2.3.3. Mulch data

To investigate the structural and hydraulic properties of the mulch in

Table 1
Distributions of soil texture, organic matter content and soil physical and hydraulic parameters for the two experimental fields. The parameters follow Normal distributions with corresponding means and standard deviation in parentheses. The texture is given in the USDA classification system.

Measurement	CA			CT		
	Layer 1 (0–3.5 cm)	Layer 2 (3.5–25 cm)	Layer 3 (25–30 cm)	Layer 1 (0–5 cm)	Layer 2 (5–25 cm)	Layer 3 (25–30 cm)
Soil texture and organic matter						
Sand (%)	46.1 (1.9)			46.9 (1.9)		
Silt (%)	38.5 (1.3)			37.4 (1.0)		
Clay (%)	15.4 (1.2)			15.7 (1.5)		
Organic matter (%)	5.1 (0.9)	3.3 (0.6)		4.0 (1.0)	3.6 (0.8)	
Number of replicates	8	8		8	8	
Soil physical and hydraulic parameters						
Bulk density ρ_b (g cm^{-3})	1.35 (0.11)	1.59 (0.11)	1.73 (0.05)	1.31 (0.14)	1.43 (0.13)	1.71 (0.09)
Field capacity θ_{FC} (%)	34.46 (3.74)	27.60 (3.15)	24.81 (2.04)	26.96 (4.00)	28.88 (3.36)	28.26 (2.42)
Number of replicates	112	96	27	112	96	27

the CA field, bulk samples were collected two times in three blocks and from the four cover crop treatments in November 2019 and March 2020, respectively. Each sample was collected on an area of 0.25 m^2 and the approximate thickness of the mulch layer was measured. Fresh subsamples of mulch of about 15 g were first dried at 65 °C for 48 h to standardize the initial water contents. They were then immersed in tap water for 16 h and subsequently drained on a 1-mm mesh sieve for 20 min. The wetted mulch was weighed and dried afterwards at 65 and 120 °C until constant weight was reached (Iqbal et al., 2013) to determine maximal and residual gravimetric water contents, respectively. The organic matter content of the collected mulch was measured with the loss-on-ignition method (Nelson and Sommers, 1996) using shredded mulch subsamples (2 cm long debris approximately) of about 5 g. The maximal and residual gravimetric water contents as well as the density measured in the field were corrected for the content of mineral soil particles.

To measure the mulch water retention curve, a third set of samples ($n = 6$) was collected in November 2020. A number of six ring cells (250-cm^3) of about 40 g (wet weight) were established with the collected mulch. The six rings were immerged in degassed water for 16 h and subsequently drained on a 1-mm mesh sieve for 20 min, before they were mounted on automated sensor units with integrated tensiometers (HYPROP version 2015, UMS GmbH, Munich, Germany). Water tension in each unit was measured at two levels of a sample with two tensiometer shafts for six days. Twice a day, the units were weighed to measure water loss through evaporation. The measurements from the two tensiometer shafts were collected until the uppermost part of the mulch (2.5 cm) dried, as this was considered representative of a 2.5-cm high layer of mulch. After six days, the rings were detached from the units and dried at 105 °C for 24 h in order to determine dry weights and estimate mulch water content under the measured tensions. Each of the water retention curves from the uppermost 2.5 cm of mulch was fitted by least-squares method to the exponential model introduce in Eq. (6) in the interval of water tension 0–10 cm.

2.3.4. Statistical analyses of field measurements

The measurements of soil bulk density and field capacity were analyzed with the statistical software R version 4.0.2 (R Core Team, 2020). The measurements were individually fitted to linear mixed-effect models with the lme4 package (Bates et al., 2015). The interaction between cropping system, sampling time, and sampling depth was considered as a fixed effect while block and cover crop treatments were included as random effects. This allowed a pair-wise comparison between the combinations of system type, sampling time and sampling depth, while considering that some variation in the bulk density and field capacity may be due to variation between blocks and cover crop treatments.

The fifth set of measurements taken in 2019 was discarded from the analysis as well as the ones from the plough pan (25–30 cm depth) because of missing samples and measurements for certain soil depths and field areas.

Similarly, the measurements of maximal and residual water contents of mulch along with mulch bulk density were fitted to linear mixed-effect models, with sampling time as fixed effect and block and cover crop treatments as random effects.

The quantile-quantile and residual plots of all mixed-effect models were visually assessed. The pairwise comparisons between the different treatments were adjusted for multiplicity using the single-step approach (Hothorn et al., 2008).

2.4. Test of the mulch module against experimental data

To test the new Daisy mulch module, the soil column experiments from Aslam et al. (2018) were used. In these experiments, maize and dolichos residues were placed on top of 25-cm soil columns at a density of 758 g m^{-2}. The soil columns were composed of two horizons sampled at two different depths – 0-5 and 5–25 cm – on an experimental site of INRAe, Versailles, France. After application of both s-metolachlor and glyphosate at doses of 1.04 and 1.29 kg active ingredient ha^{-1}, respectively, the soil columns were subject to two different artificial rainfall regimes with distilled water, namely low and frequent (LF-R) or high and infrequent regime (HI-R). All soil physical properties and details about rainfall regimes and laboratory conditions were retrieved from Aslam et al. (2018). The different organic matter pools of the mulch were described in Daisy as different AOM pools with specific C:N ratios, solubilisation rates to the DOM pool and assimilation yields by SMB2 according to Iqbal et al. (2014) and Garnier et al. (2003).

Table 2 gives an overview of the mulch and pesticide parameterization in Daisy. The value ranges of pesticide half-life time (DT50) and sorption were retrieved from EFSA reports (EFSA, 2004, 2015). With a mulch thickness of 3 cm, the decompose height factor was set to 0.6 cm to fit a 20 % initial proportion of dry mass in direct contact with the soil (Aslam et al., 2018). The measured maximal and residual water contents (see Section 2.3.3) were used in the parameterization. The mulch specific area index and extinction coefficient for mulch cover calculation (Eq. (2)) were taken from the study of Macena et al. (2003) where these values were measured and estimated for millet.

Five soil parameters of the van Genuchten-Mualem model of soil hydraulic properties (Mualem, 1976; van Genuchten, 1980) (Table S3

Table 2
Mulch module calibration: fixed and calibrated parameters of the mulch and pesticides s-metolachlor and glyphosate. DM stands for dry mass, AOM for added organic matter pool.

	Parameter name and unit	Description	Value (range)
Fixed parameters	SpMAI (m^2 kg^{-1} DM)	Area of soil covered by 1 kg of mulch	3.9[2]
	γ (−)	Factor of the specific area index	0.45[2]
	K_{MM} (g C cm^{-3})	Michaëlis-Menten constant for AOM degradation	0.000455[1]
	K_{MP} (g C cm^{-3})	Michaëlis-Menten constant for pesticide degradation	0.000455[1]
	W_M (g g^{-1} DM)	Maximal gravimetric water content of the mulch	2.25 (5.59 ± 1.10)[5]
	α (−)	Mulch propensity to water recharge	1.2 (0.5–2)[3]
	k (cm^{-1})	Exponential water retention curve parameter	0.113 (0.097 ± 0.027)[5]
	f_e (−)	Factor of the downwards Darcy water flow from mulch to soil	0.4 (0–1)[3]
Calibrated parameters	Si (%)	Saturation index for wash-off	4 (1–99)[3]
	$DT50_{surface}$, $DT50_{mulch}$, $DT50_{soil}$ (days)	Half-life time on surface, mulch and in soil (assumed equal in the study)	S-metolachlor: 9.6 (7.6–37.6)[4] Glyphosate: 140.6 (3.7–160.5)[4]
	Kd (mL g^{-1})	Linear sorption coefficient	S-metolachlor: 40.9 (1.3–55.8)[4] Glyphosate: 752.9 (5–811)[4]
	Ep (h^{-1})	Exchange rate of pesticide between mulch water and rainwater	S-metolachlor: 0.4 (0–1.5)[1] Glyphosate: 0.8 (0–1.5)[1]

[1] From or estimated from Aslam et al. (2018); Iqbal et al. (2013); Garnier et al. (2003).
[2] Macena et al. (2003).
[3] Based on Aslam et al. (2018); Iqbal et al. (2014, 2013).
[4] EFSA (2015, 2004).
[5] Estimated from measurements.

and Fig. S1 in supplementary material) were hand fitted for the two regimes given the parameters from Aslam et al. (2018). The n parameter was found to differ between the two regimes. This was attributed to differences in the soil packing during the establishment of the soil columns and effects on the pore-size distribution (van Genuchten, 1980).

A total of 8 mulch and pesticide parameters (Table 2) were automatically estimated via inverse modelling with the shuffled complex evolution algorithm developed at the University of Arizona (SCE-UA) (Duan et al., 1994). The simulated and measured contents of water and pesticide in mulch and the content of s-metolachlor in soil for the HI-R regime in Aslam et al. (2018) were used. Due to analytical issues, <6 % of the applied glyphosate could be measured in the soil by Aslam et al. (2018) during their experiment. Therefore, the glyphosate parameters were not estimated using the measurements of glyphosate concentrations in soil.

A specific value for the parameter Ep (Eq. (9)) was estimated for s-metolachlor and glyphosate separately, as this relates to the sorption capacity of pesticides to the mulch residues in Daisy. The best fit was defined by the lowest root mean square error (RMSE, Eq. (10)). The parameterization was subsequently tested under the LF-R regime.

$$RMSE = \sqrt{\frac{\sum_{i=1}^{N} (x_i - \hat{x_i})^2}{N}} \quad (10)$$

where x_i and $\hat{x_i}$ are the measured and simulated data points, respectively, and N the total number of measurements.

2.5. Uncertainty and sensitivity analyses of Daisy

2.5.1. Parameters and uncertainty

Five sources of parameter uncertainty in the modelling procedure were considered (Table 1 and Table 3): *i)* structural and hydraulic properties of soil and mulch, *ii)* density of measured drain-connected biopores, *iii)* pesticide physical and chemical characteristics, *iv)* mulch biological properties related to residues decomposition to investigate the effect of microbial activity on pesticide dynamics in mulch, and *v)* weather conditions to reflect weather variability. The distribution of mulch and pesticide parameters, along with drain-connected biopore density and weather series, were common to both CA and CT cropping scenarios, while the soil parameters had specific distributions under both scenarios.

The drain-connected biopore density (Table 3) was set to follow a uniform distribution with bounds of 0.1 and 14 m^{-2} based on the measured average density of 7 ± 0.7 (standard error) smoke-emitting biopores m^{-2} in CA. This range was used for both CA and CT to investigate the effect of low and high biopore densities under each cropping scenario. Yet, because ploughing in CT disconnects such biopores from the surface once to twice a year, connections are rather made between drains and the plough pan (i.e. about 30 cm depth) in CT, as observed in field experiments (Petersen et al., 1997; Nielsen et al., 2015). Hence, while the density range was common to both systems, under CT, half of the biopores were set to start at the soil surface and the other half at 30 cm depth.

Table 3
Distributions of mulch, pesticide and weather parameters used in uncertainty analysis. These parameters were common to CA and CT. The parameters follow Normal distributions with corresponding means and standard deviations in parentheses or uniform distributions indicated with lower and upper bounds.

Mulch parameters	
α (−) *uniform*	0.25–2[1]
W_M (g g^{-1} DM) *normal*	5.59 (1.10)[2]
k (cm^{-1}) *normal*	0.097 (0.027)[2]
Si (%) *uniform*	1–99
Factor exchange (−) *uniform*	0–1
K_{MM} (mg C kg^{-1} soil) *uniform*	0–350[1]
Drain-connected biopore density at the soil surface (m^{-2}) *uniform*	0.1–14[2]
Pesticide parameters *uniform*	
Mulch, soil and surface DT50 (days)	0.5–300
Log_{10} Koc (mL g-1)	1–4
Ep (h^{-1})	0–1.5
K_{MP} (mg C kg^{-1} soil)	0–350[1]
Weather parameter: starting year (−) *uniform (discrete)*	1962–4954

[1] Aslam et al. (2018), Findeling et al. (2007), Garnier et al. (2003). [2]Estimated from measurements.

The mulch maximal water content and k, the parameter of the exponential water retention curve (Eq. (6)), were assessed as normally distributed from measurements by visual assessments of histograms. The propensity of mulch to water recharge α (Eq. (7)) was set to vary between 0.25 (Findeling et al., 2007) and 2 (Aslam et al., 2018), thereby representing a range for water interception between about 15 and 80 %.

Mulch, soil and surface DT50 (as differentiated in Daisy to make it possible to consider surface dissipation via e.g. volatilisation) were assumed to be equal in both CA and CT. DT50 values along with linear sorption constants to organic carbon, Koc, were assigned large ranges to cover a broad spectrum of pesticide physical-chemical properties. The mass exchange rate of pesticide in the mulch (Eq. (9)) was set to vary between 0 and 1.5 h^{-1}, based on the mulch module experiment from Aslam et al. (2018) where the optimal value was found to be 1.2 h^{-1} for glyphosate, which is known to be weakly sorbing to organic carbon.

The bounds of the K_M parameters for mulch (K_{MM}) and pesticide (K_{MP}) (Eq. (4)) were fixed at 0 and 350 mg C kg^{-1} soil (Garnier et al., 2003), respectively, and converted into g C cm^{-3} using the soil surface bulk density.

The weather data used to run Daisy simulations with a 5-year crop rotation was selected based on a random discrete starting year within a 3000-year generated weather series (2.6.2.2).

2.5.2. Monte Carlo simulations

To cover a large range of soil hydraulic properties, the pedotransfer function 3 from the program Rosetta (Schaap et al., 2001) was utilized using the measured texture, the bulk density, and their respective uncertainty (Table 1). A number of 5050 combinations of sand, silt and clay contents and bulk density values were randomly sampled and given to Rosetta to predict the corresponding Mualem van Genuchten parameters (Mualem, 1976; van Genuchten, 1980) and produce water retention and hydraulic conductivity curves.

Using the soil hydraulic properties calculated by Rosetta and the parameter distribution in Table 3, 5050 Monte Carlo simulations were run under each cropping scenario. Parameters following a normal distribution were randomly sampled. The uniformly distributed parameters were pseudo-randomly sampled using the Latin hypercube sampling method, to ensure good coverage of the parameter spaces. The programming language Python was used to generate the 10,100 setup files with the Python package PyDaisy (Gudbjerg, 2019). Each simulation was run for 8 years to include a warm-up period of 3 years, which ensured realistic initial soil water contents. About 1 % of the simulations crashed, due to specific combinations of soil parameter values e.g., combinations of low alpha values from the water retention curve and high n parameter values from the hydraulic conductivity curves, increasing the air entry point while decreasing the unsaturated hydraulic conductivity. The final number of simulations successful in both CA and CT was 4939. The parameter spaces of these simulations were reasonably following the original distributions. Each of the 4939 setups had the same values for the weather, mulch, pesticide and drain-connected biopore density parameters in CA as in CT.

The load of pesticide leaving the topsoil by leaching during the full 5-year rotation as calculated by Daisy was considered as well as the mass of pesticide degraded both in the mulch, the uppermost soil layer (0–3.5 cm), and the topsoil (0–30 cm). Both leaching and degradation amounts were compared to the applied dose and expressed as percentages.

2.5.2.1. Numerical soil profiles and field management. Daisy simulates water and solute transport in soil based on the description of soil columns. For each cropping scenario, a 1-dimension soil profile composed of five different soil layers was set up (Table 1), using the corresponding measurements from the topsoil (0–30 cm). A common subsoil (30–200 cm) was added from a well-studied drained field site (Rørrendegård, Denmark, Nielsen et al. (2015), Table S1 in supplementary material). The drain depth was set at 110 cm and the drain spacing at 16 m. The columns were parameterized with drain-connected biopores and matrix-terminated biopores. The full description can be found in Table S5. In CT, drain-connected biopores starting at the soil surface or under the plough pan (30 cm depth) were described. In CA, drain-connected biopores were all starting at the surface.

Crop rotation and managements, fertilization needs, and pesticide application windows were defined by local agricultural consultants. A 5-year crop rotation *winter wheat-spring barley-winter wheat-spring barley-winter rape* was set up in Daisy for both CA and CT, with oilseed radish cover crops between winter wheat and spring barley. The rotation included an additional cover crop between the first spring barley and the second winter wheat in CA only. As Daisy does not have an oilseed radish parameterization, winter rape was used as a cover crop.

Ploughing down to 25 cm and harrowing at 5 cm depth were described in the CT management, while CA management did not include any tillage operation. Only grains were removed at harvest, with straw and leaves left on the field as residues thereby forming a mulch. For the cover crop, everything was left on the field, simulating chemical termination.

In CT, crop residues were incorporated in the topsoil later on through tillage, while in CA the formed mulch was left on the surface to decompose or become bioincorporated over time. The residues of terminated cover crops were added to the mulch layer. The same pesticide was applied once on each crop at 100 g ha^{-1} (active ingredient) but within different windows. The field management description is shown in Table S2. All field operations were conditional to soil trafficability i.e., soil pF $\geq$ 1.7 and soil temperature $>$ 0 °C at 10 cm depth, to avoid pesticide application on wet and frozen soil.

2.5.2.2. Upper and lower boundary conditions. A 3000-year weather series generated for the Danish climate starting in 1962 and ending in 4963 was used as upper boundary conditions. The weather series published by Rasmussen et al. (2018) is based on 30-year long weather measurements taken at Copenhagen Airport between 1983 and 2013. The 3000-year dataset includes hourly rainfall, generated with the stochastic rainfall model RainSim V3 (Burton et al., 2008), as well as daily air temperature, wind speed, humidity and global radiation, generated with the Climatic Research Unit weather generator (Kilsby et al., 2007) using their statistical relationship with rainfall. Rainfall follows yearly, monthly, daily and hourly real weather characteristics but does not present long-term trends like climate change.

The lower boundary conditions in the Daisy simulations consisted of a 200-cm-deep aquitard with a saturated hydraulic conductivity, K_S, of 0.010 cm h^{-1}, and a constant pressure potential of 220 cm at its bottom, for a realistic setup of the investigated fields and considered subsoil (Styczen et al., 2004).

2.5.3. Global sensitivity analysis (GSA)

A GSA would require a tremendous amount of computing time with a highly parameterized model like Daisy (N(2 + x) simulations with N the number of samples and x the number of parameters, Saltelli et al., 2008). Meta-models were therefore developed using the outputs from the Monte Carlo simulations as described in Al et al. (2019). Eight parameters retrieved from the simulations were included in the analysis: the total precipitation amount over the 5-year rotation, the five water content values in the uppermost soil layer (0–5 cm) at the pesticide application time, along with the two leaf area index (LAI) values of spring barley at application time, as only spring barley showed a positive LAI during application (Table S6). In addition, the Ks and bulk density of the three topsoil layers were included in the set of parameters. This created 4 datasets consisting of 4939 simulations with 25 parameters and 2 pesticide loss outputs (leaching and degradation). The different parameters were assumed independent. The datasets were first standardized by centering and scaling each parameter. This allowed having homogeneous data ranges regardless of the units, with parameter means of 0 and standard deviations of 1.

For pesticide degradation, a linear-regression meta-model was fitted on the input parameters for the prediction of degradation, and the standardized regression coefficients, SRCs (Saltelli et al., 2008), were computed based on Eq. (11):

$$SRC_p = w_p \frac{\sigma_{xp}}{\sigma_y} \tag{11}$$

where w_p is the weight of parameter p in the linear-regression model, σ_{xp} the standard deviation of the values of parameter p, and σ_y the standard deviation of the mass of pesticide degraded in the mulch and soil surface layer over the 5 years of simulation.

For pesticide leaching, the linear-regression meta-models were found to perform badly in predicting leaching ($R^2 < 0.7$). A modified version of the code from the GSA toolbox (https://github.com/gsi-lab/easyGSA) were used to train artificial neural networks meta-models on the previously introduced Monte Carlo simulations (2.6.2), to predict the total load of pesticide leaching from the topsoil. Training and validation of the meta-models were conducted on 90 % and 10 %, respectively, of each dataset originating from the Monte Carlo simulations. Sobol sensitivity indices were subsequently computed, including both first-order (Si, Eq. (12)) and total-order (STi, Eq. (13)) Sobol indices.

$$Si = \frac{V[E(Y|Xi)]}{V(Y)} \tag{12}$$

where *Xi* refers to a specific input parameter and *Y* to the output variable i.e., pesticide leaching from the topsoil over the 5 years of simulation. The numerator corresponds to the variance of the conditional expectation i.e., the expectation of *Y* for specific values of *Xi*. Sis allow to capture the full range of variation of each input parameter and its effect on the output variable (Saltelli et al., 2008). The higher the Si, the more influential the parameter, and the more crucial it is to find its accurate value.

$$STi = \frac{E[V(Y|X_{\sim i})]}{V(Y)} \tag{13}$$

where $X_{\sim i}$ refers to all input parameters but one, as it investigates the effect of fixing *Xi*. The numerator corresponds to the expectation of the conditional variance i.e., the variance of *Y* when *Xi* is fixed. STis capture the variation in the output variable induced by the interaction of each input parameter with the other parameters (Saltelli et al., 2008). STis thus determine the influence of the parameter on other parameters and the effect of this influence on the output variance. The lower the STi, the less interaction effects with other parameters, and the less effect on the output variance if the parameter is fixed to any value within its range of variability.

Estimates of the Sobol sensitivity indices were calculated with the neural-network meta-models. To do so, 50,000 Monte Carlo simulations were run with each meta-model. The Jansen's estimators of Sis and STis were used as suggested by Saltelli et al. (2010).

3. Results and discussion

3.1. Soil physical properties

Soil bulk density was consistently lower in the surface layer

compared to the deeper layer (Fig. 2A). In CA, this difference was significant for all sampling dates (all *p*-values <0.01). The highest density was measured at 15 cm depth in November 2018 with a mean density of 1.65 g cm^{-3} (95 % Confidence interval: 1.60, 1.70) g cm^{-3}. At this depth, the densities in CA were significantly higher than in CT, except in May 2019 (p-value = 0.149), where the average in CT was 1.46 (95 % CI: 1.40, 1.51) g cm^{-3} and 1.55 (95 % CI: 1.50, 1.60) in CA. These results were in line with those of Heard et al. (1988), who observed a significantly higher bulk density in the soil layer between 7.5 and 23.5 cm depth under no-till compared to other treatments where tillage was conducted, in silty soils.

The lowest density was measured in October 2017 in the surface layer of the CT field, with a mean density of 1.21 (95 % CI: 1.16, 1.26) g cm^{-3} as expected for a recently tilled field. In CT, the bulk density significantly increased from October 2017 to June 2018 (p-value = 0.043), which can be explained by mechanical and hydraulic stresses occurring during the winter due to soil weight and precipitation events (Bauer et al., 2015). The density decreased again in November 2018 in both the surface and 15-cm deep layers, although this decrease was borderline significant only (*p*-value = 0.051).

In Fig. 2B, field capacity ranged from 25 to around 40 % in the surface layer, and was always significantly higher in CA than in CT (all p-values <0.01). At 15 cm depth, there was no difference between the two systems (all p-values >0.7). The strong difference in the surface layer was thus attributed to the increased organic matter content in CA in contrast to CT (Table 1). Higher field capacity and bulk density values implied that less air space was available in the soil surface in CA for immediate water infiltration. The two soil layers had significantly different field capacities for all sampling dates in CA (all p-values <0.01) with higher values in the surface layer. In CT, the two layers were only significantly different in June 2018 (p-value = 0.034), where the mean field capacities were 26.60 (95 % CI: 24.74, 28.45) % and 29.94 (95 % CI: 28.09, 31.79) % in the surface and the 15-cm deep layers, respectively.

3.2. Mulch physical properties

The mulch maximal water content was significantly lower for mulch samples collected in March compared to December (p-value <0.001) with mean water contents of 4.77 ± 0.17 (standard error) and 6.00 ± 0.22 g g^{-1}, respectively. Likewise, the residual water content was lower for mulch sampled in March compared to December (p-value <0.001) with mean values of 0.022 ± 0.002 and 0.041 ± 0.002 g g^{-1}, respectively. With a period of 4 months between the two sampling campaigns, the mulch residues were subjected to weathering effects and biological decomposition which strongly affected the structure of the residues by reducing the particle size. In their study investigating the water storage characteristics of different plant tissues, Iqbal et al. (2013) demonstrated that the water retention capacity of plant residues was reduced with lower particle size of the mulch residues. In addition, they reported that the maximal water content increased with a higher degree of decomposition, which could be explained by an enhanced porosity of the plant material due to the increased presence of cavities on their cell walls. Although their measurements relate to the water retention of plant particles, their results for residual water contents for undegraded wheat straw were similar to those measured in the present study for mulch retention. Their maximal water contents were considerably smaller (2.33 ± 0.46 g g^{-1} on average for wheat) however. This could be anticipated as an in-between particles retention of water is expected in a mulch where particles are superposed.

The mulch bulk density measurements in the present study had substantial variation across samples and over time. However, the difference between the two dates with mean densities of 16.11 ± 2.22 and 14.01 ± 2.22 g L^{-1}, respectively, was not significant (p-value = 0.36).

Fitting the mulch water retention data to an exponential model resulted in the determination of a mulch water retention curve (Fig. 2C).

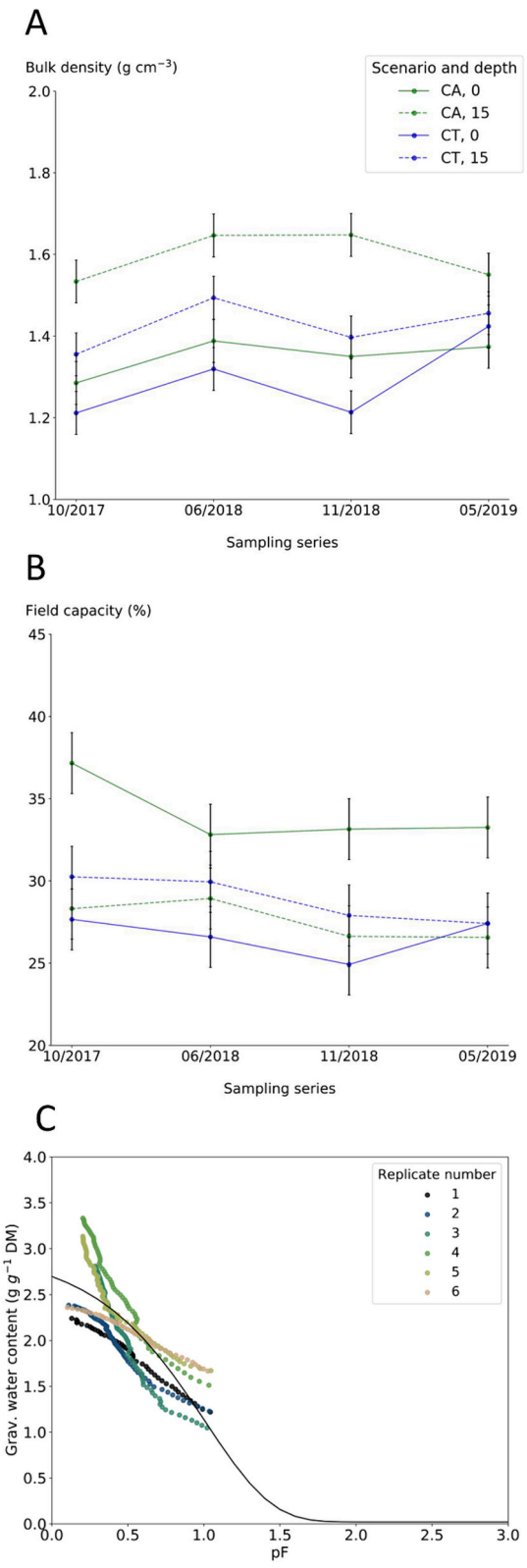

Fig. 2. A: Measured soil dry bulk density. B: Field capacity at four time points between 2017 and 2019 under the two cropping systems conservation agriculture (CA, green) and conventional tillage (CT, blue), with 95 % confidence intervals. The unbroken lines correspond to samples taken at the soil surface (0–3.5 cm), and the dotted lines to samples taken at a soil depth of 15 cm. C: Measured mulch water retention capacity (dots) and average modelled exponential retention curve (line). The different colours represent different replicates.

The drying process of the mulch up to pF 1 was reasonably well described by the exponential model, while water content for larger pF might have been underestimated. Three replicates had a particularly high water content near saturation (at pF 0) compared to the modelled water content. This could be due to the variation in the mulch packing in each ring cell as well as the measurement instability of the tensiometer shaft. The average value of the k parameter was estimated to be 0.097 ± 0.01 cm^{-1}.

3.3. Testing of the mulch module

Using published experimental data, 8 mulch and pesticide parameters along with 6 soil parameters could be estimated based on the results for the HI-R regime (Table 2, Table S3 and Fig. S1). The RMSE for soil water content was 0.02 cm cm^{-3} (Table S4). For mulch water, s-metolachlor and glyphosate contents the RMSE were 0.254 g g^{-1}, 0.013 g m^{-2} and 0.017 g m^{-2}, respectively. For s-metolachlor content in soil, the RMSE was 0.011 g m^{-2} (Table S4).

Using the fitted parameters, Daisy satisfactorily simulated water and pesticide dynamics in mulch, as well as pesticide content in soil under the HI-R regime (Fig. 3). This confirmed the suitability of the parameter ranges (Table 2). Under the LF-R regime, the simulated mulch water content was approximately 4 times lower than under HI-R. These simulated water contents appeared greatly underestimated when compared to measurements (Fig. 3, RMSE of 0.882 g g^{-1} in Table S4). This could first be explained by the description of the mulch as one layer. With the current description, the amount of water not intercepted by the mulch reaches the soil; with a two-layer structure such as in PASTIS, part of this water would be first intercepted by the lower part of the mulch, leading to an overall greater interception and mulch water content. The values for the water retention curve parameter k and the mulch propensity to water recharge α could also have been better estimated to fit the observations under LF-R. The measurements under HI-R used for inverse modelling were taken before each irrigation event. Thus, the water content of the mulch right after irrigations was unknown, making the full range of water content values uncaptured by the measurements and especially the water contents of the mulch under LF-R, thereby hampering the quality of the fitted values of k and α. Setting k at a value of 0.023 cm^{-1} i.e., 5 times lower than the fitted value, showed that a satisfactory mulch water content could be reached under LF-R (RMSE of 0.290 g g^{-1}) while keeping a satisfactory description of pesticide content in mulch and soil (Fig. S3, RMSEs of 0.290 g g^{-1} for water content, 0.009 and 0.017 g m^{-2} for s-metolachlor and glyphosate contents, and 0.013 g m^{-2} for s-metolachlor content in soil).

Daisy also overestimated mulch decomposition compared to the measurements (Fig. S2) for both rainfall regimes, although the lack of observation points made a thorough comparison with measurements difficult.

The fitted value of the mass exchange parameter Ep was greater for glyphosate (0.8 h^{-1}) than for s-metolachlor (0.4 h^{-1}). This was in line with a low sorption capacity of glyphosate to organic matter and higher measured desorption rates (Aslam et al., 2018; Rampoldi et al., 2011). The estimated DT50 values were very different from that of Aslam et al. (2018) (calibrated values) due to differences in the mulch setups including the common DT50 values of pesticides in mulch and soil and the one-layer structure in the present study.

These results show that the more generalized description of the mulch module and the parameter ranges taken from the literature and from our measurements could reproduce pesticide dynamics in mulch and soil. However, for water dynamics, while the module performed well for the measurements it was fitted on (HI-R regime), the mulch water content was poorly described when tested under another set of observations (LF-R regime). Improvements are therefore needed; this requires more precise observation data. Carrying a sensitivity analysis of the newly described mulch module can help prioritize the measurements to conduct.

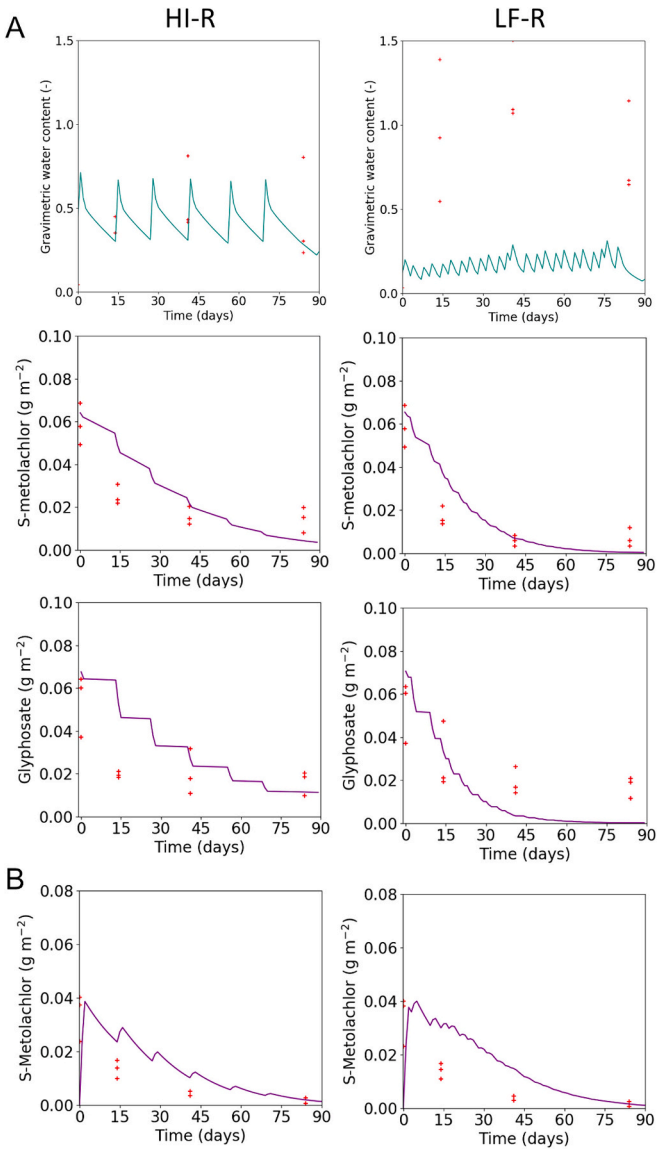

Fig. 3. Water and pesticide dynamics in mulch and soil simulated with Daisy mulch module (line) compared to measurements digitized from Aslam et al. (2018) (red cross). A: Contents of water, s-metolachlor and glyphosate in mulch for the two irrigation regimes high and infrequent (HI-R) and low and frequent (LF-R), respectively; B: Contents of s-metolachlor in the 0–5 cm soil layer for the two irrigation regimes.

3.4. Uncertainty analyses

3.4.1. Water balance

The yearly average actual transpiration in the CA and CT scenarios were very close, 185.2 ± 0.1 (standard error) and 184.2 ± 0.2 mm, respectively (Table 4), while the soil evaporation was about 26 % lower in CA due to the presence of mulch. This led to both a greater matrix and biopore net infiltration under CA and a higher percolation rate from the topsoil to the subsoil (Table 4), as also reported by Moody et al. (1963) and in the modelling study of Lammoglia et al. (2017) as effects of mulching.

Although the biopore infiltration was nearly twice as high under CA, the drain flow induced by drain-connected biopores was not higher. While the higher biopore infiltration in CA could be explained by lower hydraulic conductivities in the topsoil (Fig. S4E, Fig. S5E and Table S6) and a two-fold higher density of biopores starting at the surface, the similar drain flow showed that a larger share of water infiltrated via

Table 4
Yearly mean and standard error for actual transpiration, soil evaporation, drainage, and infiltration from the topsoil and percolation from the topsoil and bottom of the soil profile in the CA and CT scenarios. Drainage from drain-connected biopores only. Total yearly precipitation was 675.48 ± 0.76 mm.

	Pot.evap. Transp. (mm)	Actual transp. (mm)	Soil evap. (mm)	Drain flow (mm)	Biopore infiltration (mm)	Matrix infiltration (mm)	Percolation (mm)	
							from topsoil	from 200 cm depth
CA	478.5 ± 0.1	185.2 ± 0.1	105.9 ± 0.2	57.3 ± 0.4	20.1 ± 0.2	450.3 ± 0.7	352.6 ± 0.7	137.3 ± 0.5
CT	478.3 ± 0.1	184.2 ± 0.2	143.8 ± 0.1	60.4 ± 0.4	12.4 ± 0.2	431.8 ± 0.6	323.5 ± 0.7	119.1 ± 0.5

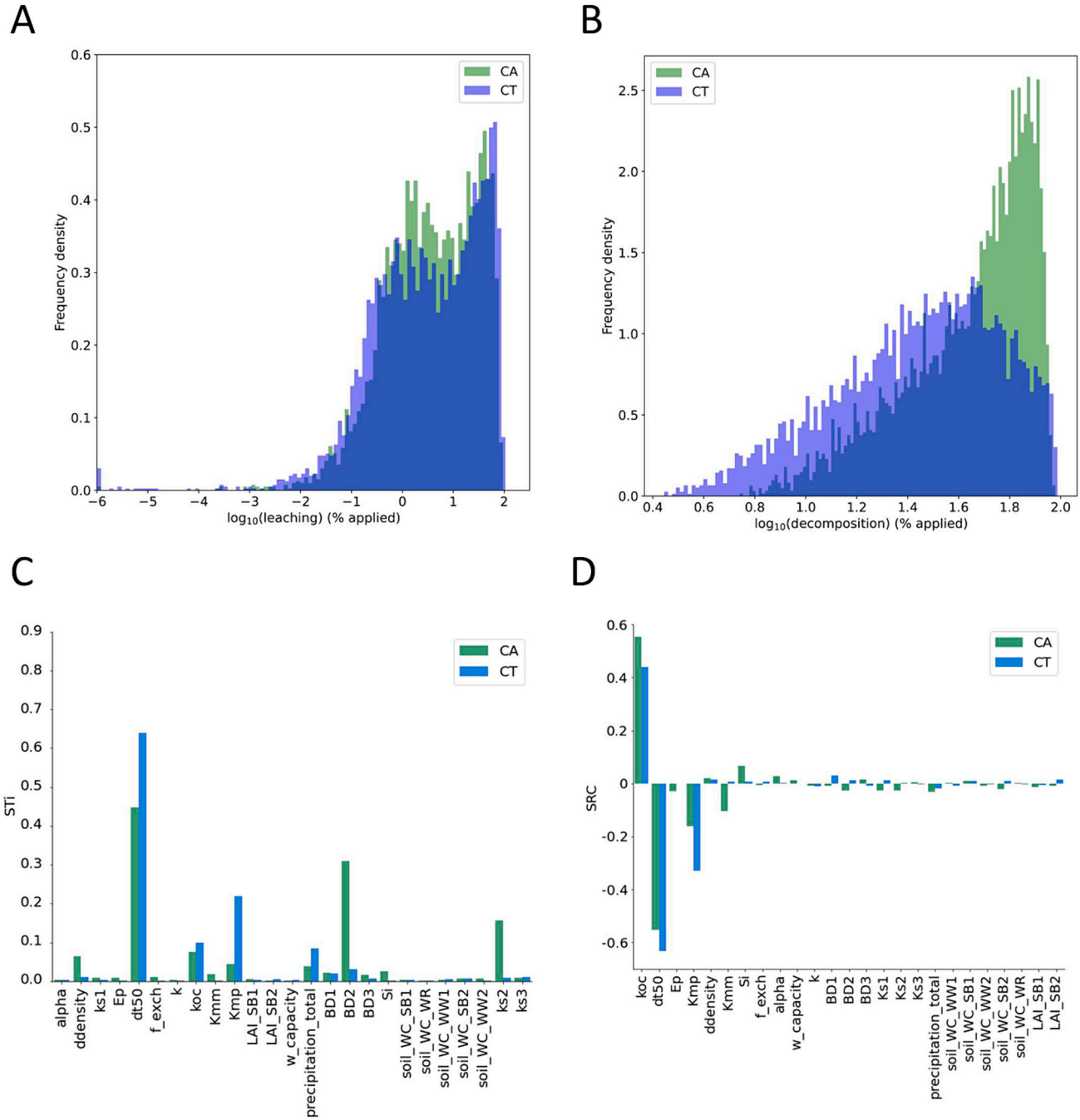

Fig. 4. A: frequency distribution of the simulated pesticide load leaching from the topsoil (0–30 cm) directly to the drains and to the subsoil (> 30 cm). B: frequency distribution of the simulated pesticide degradation in the mulch and soil surface layer (3.5 cm depth). The simulated data are given as percentage of the applied pesticide dose and log10 transformed. Null values were replaced by 10^{-6}. C: Total-order indices (STis, unitless) for the 25 parameters investigated as predictors of pesticide leaching to drains. D: Standardized regression coefficients (SRCs, unitless) for the 25 parameters investigated as predictors of pesticide degradation. Ks1, Ks2 and Ks3 refer to the predicted Ks in the corresponding soil layers. BD refers to bulk density. soil_WC_SB1, soil_WC_SB2, soil_WC_WW1, soil_WC_WW2 and soil_WC_WR refer to the soil water content (average from 0 to 5 cm depth) on the pesticide application day during the first or second spring barley, winter wheat and winter rape cultivation, respectively.

matrix-terminating biopores in CA, leading to more percolation from the bottom of the numerical soil profile (137.3 ± 0.5 mm in CA against 119.1 ± 0.5 mm in CT).

3.4.2. Pesticide leaching and degradation

The distributions of the pesticide load leaching from the topsoil or directly from the surface to the drains were very similar for the two scenarios, with only a slightly lower mean in CA of 13.9 ± 0.3 % (standard error, % of the applied dose) compared to 14.9 ± 0.3 % in CT (Fig. 4A). Pesticide degradation in the mulch and uppermost 3.5-cm soil layer was significantly higher in CA than under CT, with mean degradations of 49.7 ± 0.3 and 35.2 ± 0.3 % of the applied dose, respectively (Fig. 4B). When considering the whole ploughing layer (0–25 cm) the degradation was slightly higher in CT (Fig. S6) with mean degradations of 72.2 ± 0.3 compared to 66.9 ± 0.3 % in CA. The difference was due to the interception of some pesticides in the upper part of the mulch, where degradation is assumed negligible. These results show that mechanical incorporation of residues in the ploughing layer in CT promoted the biodegradation of pesticides, but that in CA, this could be counterbalanced by interception in the upper part of the mulch where degradation does not occur. Interception in mulch could also be the reason for the slightly higher mean leaching under CT.

Pesticide degradation in the soil might be overestimated as Daisy does not account for observed negative effect of sorption on degradation (Alletto et al., 2010; Fomsgaard, 2004). As a potential improvement of the model, degradation could be reduced when pesticides are sorbed to e.g. clay as compared to pesticides in the water phase.

3.5. Sensitivity analyses

The distribution in terms of mean and standard error of all variables used in the sensitivity analysis are provided in Table S6.

For pesticide leaching from the topsoil, the meta-models showed R^2 on the test sets ranging from 0.98 to 0.99 and from 0.65 to 0.71 for pesticide degradation in the mulch and surface layer. The two most influential parameters of leaching for both CA and CT, as estimated by these meta-models and the calculated STis (Fig. 4C), were the DT50 and the linear sorption coefficient to organic carbon Koc. Pesticide leaching in CT was also highly sensitive to the Michaëlis-Menten constant for pesticide degradation by soil microbes K_{MP}. In CA, pesticide leaching was generally found sensitive to more parameters including both pesticide, mulch and soil parameters (Fig. 4C). The soil bulk density was of great influence as well as the K_S, highlighting the necessity to carefully measure these variables. The density of drain-connected biopores, the mulch saturation index Si and the Michaëlis-Menten constants for pesticide and mulch degradation were also influential although to a lower extent. The importance of bulk density and K_s, and in particular in the soil layer 3.5–25 cm, was most likely related to their potential to increase or reduce the occurrence of biopore flow by soil saturation, as this layer had on average a significantly higher density than the surface layer (Fig. 2) and a lower K_s (Fig. S4 and Table S6). In CT, the sensitivity index of Ks was close to 0 indicating low influence of this parameter.

These results confirm the findings of the review from Dubus et al. (2003), in that predictions of pesticide leaching have been reported sensitive to sorption and degradation parameters but also hydrological parameters such as K_S. In the review of Brown and van Beinum (2009), the measured seasonal loss of pesticide to drains was significantly related to the pesticide sorption capacity to soil and soil DT50.

The parameter DT50 was also greatly influential for pesticide degradation (Fig. 4D), but contrary to pesticide leaching, degradation appeared equally sensitive to the parameter Koc.

Pesticide degradation in soil or mulch depends on both the amount of pesticide transferred from the mulch to the soil and the degradation rate. The former depends on the water content at which wash-off can occur i.e., Si, and the latter on the microbial factor f_b, which in turn depends on the K_{MP} factor, as it controls the increase in f_b. Si was shown to influence degradation positively in mulch and soil, most likely by hampering wash-off (Fig. 4D), while K_{MP} had a negative effect by slowing down the degradation rate of pesticide. The sensitivity analysis of Aslam et al. (2018), performed by following the "one-factor-at-a-time" method, also showed that both mulch degradation and wash-off were highly sensitive to the parameter Si.

The STi of K_{MM} was close to 0 for leaching whereas it was the fourth most influential parameter for degradation in CA. This was because the SMB2 pool increases with mulch degradation, which in turns increases pesticide degradation.

With very low STi values compared to the other parameters, the hydraulic mulch parameters introduced in the present work, namely the mulch propensity to water recharge, α, the water-exchange factor between mulch and soil, fe, the water retention curve parameter, k, and the maximal water content, appeared to have little influence on pesticide leaching. Their value close to 0 implied that they could be fixed to the measured average values or the values found in the literature without affecting leaching. These parameters were also found to have little effect on pesticide degradation (Fig. 4D), which highlighted the greater importance of the parameter Si, defining the lowest water content at which wash-off starts to occur, over the parameters affecting the amount of wash-off such as Ep, α and k, as also seen during the testing of the mulch module in Section 3.3. Similarly, the bulk density and K_S were found more influential than the density of drain-connected biopores for leaching. This meant that the triggering of biopore flow was more important than the actual density of biopores. This has previously been shown by Holbak et al. (2022) who used inverse modelling of observations of water flow and pesticide concentrations in drains to estimate the density of drain-connected biopores. The resulting estimate had a confidence interval range from 0.004 to 2507 m^{-2}.

Total precipitation over the 5-year rotation appeared to influence leaching but to a lower extent than pesticide and soil parameters, while it was nearly non-influential for degradation. In their modelling study with the MACRO model, Nolan et al. (2008) showed that cumulative rainfall influenced leaching to drains, in particular for a moderately mobile and moderately persistent pesticide. But their study highlighted that the timing of rainfall events and their intensity in relation to the day of application were of greater influence.

When comparing the STis to the first-order indices (Fig. S7), the parameters Si, K_{MM} and bulk density appeared to have a small interaction with other parameters. These interactions could partly explain the unsuitability of the linear regression models for predicting pesticide leaching, compared to neural networks.

4. Conclusion

Under the assumptions of instantaneous pesticide sorption, co-metabolic degradation, and input parameter distributions, the uncertainty analysis with Monte Carlo simulations resulted in close distributions of leached loads of pesticide from the topsoil between the CA and CT scenarios – with a slightly lower mean in CA than in CT –, although the density of drain-connected biopores starting at the surface was two-fold higher in CA than in CT. The degradation of pesticide showed vertical heterogeneity: while degradation in the mulch and soil surface layers was found significantly higher in CA, CT was characterized with a greater degradation when considering the whole ploughing layer due to mulch incorporation by tillage. The quantity not degraded in CA compared to CT was found to be retained in the mulch layer not in contact with the soil i.e., where degradation is assumed negligible.

The sensitivity analysis identified 7 parameters out of 25 as the most critical for pesticide leaching and degradation given the input parameter distributions. It showed that the mulch hydraulic parameters could be fixed to any value within their distribution without influencing pesticide degradation and leaching. In contrast, the microbial factors of mulch and pesticide degradation, mulch saturation index, as well as soil hydraulic properties need to be accurately estimated in order to improve

the accuracy and precision of estimated pesticide leaching and degradation distributions. This raised the need for conducting further experimental studies to better describe degradation in both mulch and soil and thereby improve the estimated uncertainty in pesticide leaching modelling. In particular, field and laboratory studies would allow to follow the degradation of mulch as affected by different pedoclimatic conditions but also pesticide fate as affected by the residue type and decomposition of cover and main crops.

A better estimation of the 7 identified parameters may modify the conclusions regarding the distribution of leached loads in CA and CT. In addition, as matrix-terminating biopores played an important role in water infiltration, their contribution as well as that of the subsoil in general to water and pesticide transport to drains should be considered in future works.

CRediT authorship contribution statement

Jeanne Vuaille: Formal analysis, Investigation, Methodology, Visualization, Writing – original draft. **Per Abrahamsen:** Formal analysis, Investigation, Methodology, Software, Supervision, Writing – review & editing. **Signe M. Jensen:** Supervision, Writing – review & editing. **Efstathios Diamantopoulos:** Supervision, Writing – review & editing. **Tomke S. Wacker:** Writing – review & editing. **Carsten T. Petersen:** Supervision, Writing – review & editing.

Declaration of competing interest

The authors declare that they have no known competing financial interests or personal relationships that could have appeared to influence the work reported in this paper.

Data availability•

Software: Daisy, developed at the University of Copenhagen by Per Abrahamsen since 1995: https://daisy.ku.dk/

Open source. Implementation code: C++•

Code: The code for Daisy simulations, uncertainty and sensitivity analyses are publicly available in the following GitHub repository: https://github.com/jvuaille/Modelling-no-till-and-mulching-in-CA•

Data repository: soil and mulch measurements as well as simulation outcomes are publicly available at: https://www.doi.org/10.17894/ucph.7a8048f2-663f-44d1-be61-878ff36263df

Acknowledgments

We would like to thank the team at Agrovi for helpful advice and insight in conducting this study within the framework of the "Grønne Marker og Stærke Rødder (GMSR)" project. We would also like to acknowledge the technical help of Anja Weibel.

Funding

The study received funding from The Velux Foundation (grant number 13602) and Promilleafgiftsfonden for Landbrug.

Disclaimer

Jeanne Vuaille is currently employed at the European Environment Agency (EEA). The text in this article solely expresses the author's own views and not those of the EEA.

Appendix A. Supplementary data

Supplementary data to this article can be found online at https://doi.org/10.1016/j.scitotenv.2024.172559.

References

Abrahamsen, P., Hansen, S., 2000. Daisy: an open soil-crop-atmosphere system model. Environ. Model. Software 15, 313–330. https://doi.org/10.1016/S1364-8152(00)00003-7.

Abrahamsen, P., Gjettermann, B., Hansen, S., 2010. Initializing organic matter pools 8.

Al, R., Behera, C.R., Zubov, A., Gernaey, K.V., Sin, G., 2019. Meta-modeling based efficient global sensitivity analysis for wastewater treatment plants – an application to the BSM2 model. Comput. Chem. Eng. 127, 233–246. https://doi.org/10.1016/j.compchemeng.2019.05.015.

Alletto, L., Coquet, Y., Benoit, P., Heddadj, D., Barriuso, E., 2010. Tillage management effects on pesticide fate in soils. A review. Agron. Sustain. Dev. 30, 367–400. https://doi.org/10.1051/agro/2009018.

Aslam, S., Iqbal, A., Deschamps, M., Recous, S., Garnier, P., Benoit, P., 2015. Effect of rainfall regimes and mulch decomposition on the dissipation and leaching of S-metolachlor and glyphosate: a soil column experiment. Pest Manag. Sci. 71, 278–291. https://doi.org/10.1002/ps.3803.

Aslam, S., Iqbal, A., Lafolie, F., Recous, S., Benoit, P., Garnier, P., 2018. Mulch of plant residues at the soil surface impact the leaching and persistence of pesticides: a modelling study from soil columns. J. Contam. Hydrol. 214, 54–64. https://doi.org/10.1016/j.jconhyd.2018.05.008.

Bates, D., Maechler, M., Bolker, B., Walker, S., 2015. Fitting Linear Mixed-Effects Models Using lme4, 67, pp. 1–48. https://doi.org/10.18637/jss.v067.i01.

Bauer, T., Strauss, P., Grims, M., Kamptner, E., Mansberger, R., Spiegel, H., 2015. Long-term agricultural management effects on surface roughness and consolidation of soils. Soil Tillage Res. 151, 28–38. https://doi.org/10.1016/j.still.2015.01.017.

Bollag, J.-M., Liu, S.-Y., 1990. Biological transformation processes of pesticides. In: Pesticides in the Soil Environment: Processes, Impacts and Modeling. John Wiley & Sons, Ltd, pp. 169–211. https://doi.org/10.2136/sssabookser2.c6.

Brisson, N., Mary, B., Ripoche, D., Jeuffroy, M.H., Ruget, F., Nicoullaud, B., Gate, P., Devienne-Barret, F., Antonioletti, R., Durr, C., Richard, G., Beaudoin, N., Recous, S., Tayot, X., Plenet, D., Cellier, P., Machet, J.-M., Meynard, J.M., Delécolle, R., 1998. STICS: a generic model for the simulation of crops and their water and nitrogen balances. I. Theory and parameterization applied to wheat and corn. Agronomie 18, 311–346. https://doi.org/10.1051/agro:19980501.

Brown, C.D., van Beinum, W., 2009. Pesticide transport via sub-surface drains in Europe. Environ. Pollut., Persistent Organic Pollutants in Mountainous Areas, 157, pp. 3314–3324. https://doi.org/10.1016/j.envpol.2009.06.029.

Bruun, S., Christensen, B.T., Hansen, E.M., Magid, J., Jensen, L.S., 2003. Calibration and validation of the soil organic matter dynamics of the Daisy model with data from the Askov long-term experiments. Soil Biol. Biochem. 35, 67–76. https://doi.org/10.1016/S0038-0717(02)00237-7.

Burton, A., Kilsby, C.G., Fowler, H.J., Cowpertwait, P.S.P., O'Connell, P.E., 2008. RainSim: a spatial–temporal stochastic rainfall modelling system. Environ. Model. Software 23, 1356–1369. https://doi.org/10.1016/j.envsoft.2008.04.003.

Cassigneul, A., Alletto, L., Benoit, P., Bergheaud, V., Etiévant, V., Dumény, V., Le Gac, A. L., Chuette, D., Rumpel, C., Justes, E., 2015. Nature and decomposition degree of cover crops influence pesticide sorption: quantification and modelling. Chemosphere 119, 1007–1014. https://doi.org/10.1016/j.chemosphere.2014.08.082.

Duan, Q., Sorooshian, S., Gupta, V.K., 1994. Optimal use of the SCE-UA global optimization method for calibrating watershed models. J. Hydrol. 158, 265–284. https://doi.org/10.1016/0022-1694(94)90057-4.

Dubus, I.G., Brown, C.D., Beulke, S., 2003. Sources of uncertainty in pesticide fate modelling. Sci. Total Environ. 317, 53–72. https://doi.org/10.1016/S0048-9697(03)00362-0.

EFSA, 2004. Review Report for the Active Substance S-Metolachlor (No. SANCO/1426/2001-rev. 3). EFSA.

EFSA, 2015. Conclusion on the peer review of the pesticide risk assessment of the active substance glyphosate. EFSA J. 13 https://doi.org/10.2903/j.efsa.2015.4302.

FAO, 2021. Conservation Agriculture | Food and Agriculture Organization of the United Nations [WWW Document]. Food Agric. Organ. U. N. URL. http://www.fao.org/conservation-agriculture/en/ (accessed 11.12.20).

FAO, 2022. Conservation Agriculture | Food and Agriculture Organization of the United Nations. Food and Agriculture Organization of the United Nations. https://www.fao.org/conservation-agriculture/en/.

Findeling, A., Chanzy, A., Louvigny, N.D., 2003. Modeling water and heat flows through a mulch allowing for radiative and long-distance convective exchanges in the mulch. Water Resour. Res. 39 https://doi.org/10.1029/2002WR001820.

Findeling, A., Garnier, P., Coppens, F., Lafolie, F., Recous, S., 2007. Modelling water, carbon and nitrogen dynamics in soil covered with decomposing mulch. Eur. J. Soil Sci. 58, 196–206. https://doi.org/10.1111/j.1365-2389.2006.00826.x.

FOCUS, 2001. FOCUS Surface Water Scenarios in the EU Evaluation Process under 91/414/EEC (Report of the FOCUS Working Group on Surface Water Scenarios No. EC Document Reference SANCO/4802/2001-rev.2).

Fomsgaard, I.S., 2004. The influence of sorption on the degradation of pesticides and other Chemicals in Soil. Dan. Environ. Prot. Agenc, Environmental Project No. 902 2004 78.

Garnier, P., Néel, C., Aita, C., Recous, S., Lafolie, F., Mary, B., 2003. Modelling carbon and nitrogen dynamics in a bare soil with and without straw incorporation. Eur. J. Soil Sci. 54, 555–568. https://doi.org/10.1046/j.1365-2389.2003.00499.x.

Gee, G.W., Or, D., 2002. Particle size analysis. In: Dane, J.H., Topp, G.C. (Eds.), Methods of Soil Analysis. Part 4. Soil Science Society of America, Madison, Wisconsin, pp. 255–293.

van Genuchten, M.Th., 1980. A closed-form equation for predicting the hydraulic conductivity of unsaturated soils. Soil Sci. Soc. Am. J. 44, 892. https://doi.org/10.2136/sssaj1980.03615995004400050002x.

Gudbjerg, J., 2019. pydaisy: Various helper classes to read and manipulate Daisy input and output files.
Gyldengren, J.G., Abrahamsen, P., Olesen, J.E., Styczen, M., Hansen, S., Gislum, R., 2020. Effects of winter wheat N status on assimilate and N partitioning in the mechanistic agroecosystem model DAISY. J. Agron. Crop Sci. 206, 784–805. https://doi.org/10.1111/jac.12412.
Hansen, S., Jensen, H.E., Nielsen, N.E., Svendsen, H., 1991. Simulation of nitrogen dynamics and biomass production in winter wheat using the Danish simulation model DAISY. Fertil. Res. 27, 245–259. https://doi.org/10.1007/BF01051131.
Hansen, S., Abrahamsen, P., Petersen, C.T., Styczen, M., 2012a. Daisy: model use, calibration, and validation. Trans. ASABE 55, 1317–1333.
Hansen, S., Petersen, C.T., Mollerup, M., Abrahamsen, P., Gjettermann, B., Nielsen, M.H., Styczen, M., Poulsen, R., Lørup, J.K., Yamagata, K., Butts, M., 2012b. Flerdimensional modellering af vandstrømning og stoftransport i de øverste 1-2m af jorden i systemer med markdræn (Bekæmpelsesmiddelforskning fra Miljøstyrelsen No. 138). Danish Environment Protection Agency.
Heard, J.R., Kladivko, E.J., Mannering, J.V., 1988. Soil macroporosity, hydraulic conductivity and air permeability of silty soils under long-term conservation tillage in Indiana. Soil Tillage Res. 11, 1–18. https://doi.org/10.1016/0167-1987(88)90027-X.
Henneron, L., Bernard, L., Hedde, M., Pelosi, C., Villenave, C., Chenu, C., Bertrand, M., Girardin, C., Blanchart, E., 2015. Fourteen years of evidence for positive effects of conservation agriculture and organic farming on soil life. Agron. Sustain. Dev. 35, 169–181. https://doi.org/10.1007/s13593-014-0215-8.
Holbak, M., Abrahamsen, P., Hansen, S., Diamantopoulos, E., 2021. A physically based model for preferential water flow and solute transport in drained agricultural fields. Water Resour. Res. https://doi.org/10.1029/2020WR027954 n/a, e2020WR027954.
Holbak, M., Abrahamsen, P., Diamantopoulos, E., 2022. Modeling preferential water flow and pesticide leaching to drainpipes: The effect of drain-connecting and matrix-terminating biopores. Water Resour. Res. 58, e2021WR031608 https://doi.org/10.1029/2021WR031608.
Hothorn, T., Bretz, F., Westfall, P., 2008. Simultaneous inference in general parametric models. Biom. J. 50, 346–363.
Iqbal, A., Beaugrand, J., Garnier, P., Recous, S., 2013. Tissue density determines the water storage characteristics of crop residues. Plant and Soil 367, 285–299. https://doi.org/10.1007/s11104-012-1460-8.
Iqbal, A., Garnier, P., Lashermes, G., Recous, S., 2014. A new equation to simulate the contact between soil and maize residues of different sizes during their decomposition. Biol. Fertil. Soils 50, 645–655. https://doi.org/10.1007/s00374-013-0876-5.
Jarvis, N.J., 2007. A review of non-equilibrium water flow and solute transport in soil macropores: principles, controlling factors and consequences for water quality. Eur. J. Soil Sci. 58, 523–546. https://doi.org/10.1111/j.1365-2389.2007.00915.x.
Jarvis, N., Larsbo, M., 2012. MACRO (v5.2): model use, calibration, and validation. Trans. ASABE 55, 1413–1423. https://doi.org/10.13031/2013.42251.
Kassam, A., Friedrich, T., Derpsch, R., 2019. Global spread of conservation agriculture. Int. J. Environ. Stud. 76, 29–51. https://doi.org/10.1080/00207233.2018.1494927.
Kilsby, C.G., Jones, P.D., Burton, A., Ford, A.C., Fowler, H.J., Harpham, C., James, P., Smith, A., Wilby, R.L., 2007. A daily weather generator for use in climate change studies. Environ. Model. Software 22, 1705–1719. https://doi.org/10.1016/j.envsoft.2007.02.005.
Lafolie, F., Cousin, I., Marron, P.-A., Mollier, A., Pot, V., Moitrier, Ni, Moitrier, Na, Nouguier, C., 2014. The « VSOIL » modeling platform. Rev. For. Fr. Fr. https://doi.org/10.4267/2042/56287. ISSN 0035.
Lammoglia, S.-K., Makowski, D., Moeys, J., Justes, E., Barriuso, E., Mamy, L., 2017. Sensitivity analysis of the STICS-MACRO model to identify cropping practices reducing pesticides losses. Sci. Total Environ. 580, 117–129. https://doi.org/10.1016/j.scitotenv.2016.10.010.
Levanon, D., Meisinger, J.J., Codling, E.E., Starr, J.L., 1993. Impact of tillage on microbial activity and the fate of pesticides in the upper soil. Water Air Soil Pollut. 72, 179–189. https://doi.org/10.1007/BF01257123.
Macena, F., Corbeels, M., Scopel, E., Affholder, F., Pinto, H.S., 2003. Characterising effects of surface residues on evaporation for a simple water balance model. In: 2nd World Congress on Conservation Agriculture. FEBRAPDP, Foz do Iguaçu, Brazil, pp. 522–524.
Marín-Benito, J.M., Alletto, L., Barriuso, E., Bedos, C., Benoit, P., Pot, V., Mamy, L., 2018. Pesticide fate modelling in conservation tillage: simulating the effect of mulch and cover crop on S-metolachlor leaching. Sci. Total Environ. 628–629, 1508–1517. https://doi.org/10.1016/j.scitotenv.2018.02.144.
Mollerup, M., Abrahamsen, P., Petersen, C.T., Hansen, S., 2014. Comparison of simulated water, nitrate, and bromide transport using a Hooghoudt-based and a dynamic drainage model. Water Resour. Res. 50, 1080–1094. https://doi.org/10.1002/2012WR013318.
Moody, J.E., Jones Jr., J.N., Lillard, J.H., 1963. Influence of straw mulch on soil moisture, soil temperature and the growth of corn. Soil Sci. Soc. Am. J. 27, 700–703. https://doi.org/10.2136/sssaj1963.03615995002700060038x.
Mualem, Y., 1976. A new model for predicting the hydraulic conductivity of unsaturated porous media. Water Resour. Res. 12, 513–522. https://doi.org/10.1029/WR012i003p00513.
Mueller, T., Jensen, L.S., Magid, J., Nielsen, N.E., 1997. Temporal variation of C and N turnover in soil after oilseed rape straw incorporation in the field: simulations with the soil-plant-atmosphere model DAISY. Ecol. Model. 99, 247–262. https://doi.org/10.1016/S0304-3800(97)01959-5.
Nelson, D.W., Sommers, L.E., 1996. Total carbon, organic carbon, and organic matter. In: Sparks, D.L., Bartels, J.M. (Eds.), Methods of Soil Analysis, Soils Science Society of America. Madison, Wisconsin, pp. 961–1010.
Nielsen, M.H., Petersen, C.T., Hansen, S., 2015. Identification of efficient transport pathways from the soil surface to field drains by smoke injection. Eur. J. Soil Sci. 66, 516–524. https://doi.org/10.1111/ejss.12235.
Nolan, B.T., Dubus, I.G., Surdyk, N., Fowler, H.J., Burton, A., Hollis, J.M., Reichenberger, S., Jarvis, N.J., 2008. Identification of key climatic factors regulating the transport of pesticides in leaching and to tile drains. Pest Manag. Sci. 64, 933–944. https://doi.org/10.1002/ps.1587.
Petersen, C.T., Hansen, S., Jensen, H.E., 1997. Depth distribution of preferential flow patterns in a sandy loam soil as affected by tillage. Hydrol. Earth Syst. Sci. 4, 769–776. https://doi.org/10.5194/hess-1-769-1997.
Petersen, C.T., Jensen, H.E., Hansen, S., Bender Koch, C., 2001. Susceptibility of a sandy loam soil to preferential flow as affected by tillage. Soil Tillage Res. 58, 81–89. https://doi.org/10.1016/S0167-1987(00)00186-0.
Petersen, C.T., Nielsen, M.H., Hansen, S., 2012. Quantification of drain-connected macroporous flow pathways by smoke injection. Soil Sci. Soc. Am. J. 76, 331–341. https://doi.org/10.2136/sssaj2011.0163.
R Core Team, 2020. R: A Language and Environment for Statistical Computing. R Foundation for Statistical Computing, Vienna, Austria.
Rampoldi, E.A., Hang, S., Barriuso, E., 2011. The fate of glyphosate in crop residues. Soil Sci. Soc. Am. J. 75, 553–559. https://doi.org/10.2136/sssaj2010.0105.
Rasmussen, S.B., Blenkinsop, S., Burton, A., Abrahamsen, P., Holm, P.E., Hansen, S., 2018. Climate change impacts on agro-climatic indices derived from downscaled weather generator scenarios for eastern Denmark. Eur. J. Agron. 101, 222–238. https://doi.org/10.1016/j.eja.2018.04.004.
Reichenberger, S., Bach, M., Skitschak, A., Frede, H.-G., 2007. Mitigation strategies to reduce pesticide inputs into ground- and surface water and their effectiveness; a review. Sci. Total Environ. 384, 1–35. https://doi.org/10.1016/j.scitotenv.2007.04.046.
Saltelli, A., Ratto, M., Andres, T., Campolongo, F., Cariboni, J., Gatelli, D., Saisana, M., Tarantola, S., 2008. Global Sensitivity Analysis. The Primer. John Wiley & Sons, Ltd, Chichester, UK. https://doi.org/10.1002/9780470725184.
Saltelli, A., Annoni, P., Azzini, I., Campolongo, F., Ratto, M., Tarantola, S., 2010. Variance based sensitivity analysis of model output. Design and estimator for the total sensitivity index. Comput. Phys. Commun. 181, 259–270. https://doi.org/10.1016/j.cpc.2009.09.018.
Schaap, M.G., Leij, F.J., van Genuchten, M.Th., 2001. Rosetta: a computer program for estimating soil hydraulic parameters with hierarchical pedotransfer functions. J. Hydrol. 251, 163–176. https://doi.org/10.1016/S0022-1694(01)00466-8.
Scopel, E., Triomphe, B., Affholder, F., Da Silva, F.A.M., Corbeels, M., Xavier, J.H.V., Lahmar, R., Recous, S., Bernoux, M., Blanchart, E., de Carvalho Mendes, I., De Tourdonnet, S., 2013. Conservation agriculture cropping systems in temperate and tropical conditions, performances and impacts. A review. Agron. Sustain. Dev. 33, 113–130. https://doi.org/10.1007/s13593-012-0106-9.
Styczen, M., Hansen, S., Jensen, L.S., Svendsen, H., Abrahamsen, P., Børgesen, C.D., Thirup, C., Østergaard, H.S., 2004. Standardopstillinger til Daisy-modellen. Vejledning og baggrund (No. Version 1.2, april 2006). DHI Institut for Vand og Miljø.
Suárez, L.A., 2005. PRZM-3, a model for predicting pesticide and nitrogen fate in the crop root and unsaturated soil zones: User's manual for release 3.12.2. EPA/600/R-05/111.
Vuaille, J., Daraghmeh, O., Abrahamsen, P., Jensen, S.M., Nielsen, S.K., Munkholm, L.J., Green, O., Petersen, C.T., 2021. Wheel track loosening can reduce the risk of pesticide leaching to surface waters. Soil Use Manage. 37, 906–920. https://doi.org/10.1111/sum.12641.
Wacker, T.S., Jensen, L.S., Thorup-Kristensen, K., 2022. Conservation agriculture affects soil organic matter distribution, microbial metabolic capacity and nitrogen turnover under Danish field conditions. Soil Tillage Res. 224, 105508 https://doi.org/10.1016/j.still.2022.105508.